Doppler radar-based pothole sensing using spectral features in k-nearest neighbors

Muhammad Aiman Dani Asmadi[1], Suraya Zainuddin[1], Haslinah Mohd Nasir[1], Ida Syafiza Md Isa[1], Nur Emileen Abd Rashid[2], Idnin Pasya[3]

[1]Department of Engineering Technology, Fakulti Teknologi dan Kejuruteraan Elektronik dan Komputer, Universiti Teknikal Malaysia Melaka, Melaka, Malaysia
[2]Microwave Research Institute (MRI), Universiti Teknologi MARA, Shah Alam, Selangor, Malaysia
[3]Department of Computer Science and Engineering, University of Aizu, Aizu-Wakamatsu, Ikki-Machi Tsuruga, Fukushima Prefecture, Japan

Article Info

ABSTRACT

Potholes, resulting from wear, weather, and traffic, pose a substantial road safety concern, driving up maintenance costs and government liabilities. Numerous studies have explored pothole detection systems, however, there is a limited focus on radar-based approaches. This study investigates the use of Doppler radar mounted on moving vehicles to collect asphalt road surface data, with the aim to leverage this unique perspective point. Spectral features from power spectral density (PSD) are extracted and explored by incorporating Doppler signal PSD features into a k-nearest neighbors (KNN) within a machine learning framework for road condition classification. Six KNN algorithms are applied, and results indicate that potholes exhibit distinct spectral differences characterized by higher variability, with fine KNN performing the best, achieving an accuracy rate of 95.38% on the test dataset. In summary, this research underscores the effectiveness of Doppler radar-based pothole sensing and emphasizes the significance of algorithm and feature selection for achieving accurate results, proposing the viability of radar systems and machine learning.

Corresponding Author:

Suraya Zainuddin
Department of Engineering Technology, Fakulti Teknologi dan Kejuruteraan Elektronik dan Komputer
Universiti Teknikal Malaysia Melaka
Jalan Hang Tuah Jaya, 76100 Durian Tunggal, Melaka, Malaysia
Email: suraya@utem.edu.my

1. INTRODUCTION

Recent advancements in transportation infrastructure focus on road safety and durability, with a critical challenge of pothole sensing. Potholes, depressions in road surfaces due to deteriorated asphalt and weakened soil, have global negative impacts, from compromised safety to financial burdens on government agencies. Therefore, efficient and accurate pothole sensing is vital for proactive maintenance and road safety.

For instance, in Malaysia, where road quality has declined, a collaboration between the government and Waze identified about 50,000 potholes in Selangor between 2019 and 2020. Malaysia ranked as the 12th country with the worst roads globally [1], has experienced a persistent decline in road quality, resulting in a surge in road fatalities. Furthermore, governmental bodies such as the Malaysian Public Works Department (JKR) and local authorities are responsible for road maintenance, potentially facing compensation claims due to perceived negligence in pothole management. This highlights the need for innovative pothole detection to address safety and maintenance challenges.

Various methods for pothole detection are prevalent, including vision, laser, acoustic, radar, and vibrational approaches [2]-[13]. These methods possess distinct advantages and limitations. For instance, vision and laser-based sensors may struggle in adverse conditions, while acoustic sensors offer a cost-effective solution but have difficulty distinguishing obstacles. Vibration-based sensors face challenges in detecting minor defects and suffer from battery limitations. Recent advancements in radar systems combined with artificial intelligence show a promising sensing solution for addressing this challenge. Exploration of the optimal features is crucial to improve system performance [14].

A Doppler radar can determines velocity, however, poses limitations for pothole detection due to its inability to measure depth [15]. Besides, surrounding elements often obscure echoes from the target of Doppler's signals, lead to challenges in distinguishing the target of interest [9]. The proposed work incorporating k-nearest neighbors (KNN) models, complement pothole detection by classifying road conditions, based on features extracted from Doppler radar power spectral density (PSD) plots. Six KNN algorithms enhance data-driven decision-making for pothole sensing system improvement.

The paper proceeds as follows: section 2 offers a literature review of prior research on pothole sensing and classification. Section 3 presents the method, including data collection, signal pre-processing, and machine learning. Section 4 presents the outcomes of the machine learning-powered pothole sensing system and section 5 concludes the work.

2. LITERATURE REVIEW

2.1. Pothole scanning using radar

Numerous studies have utilised radar systems on moving vehicles to collect pothole data, exploiting the effectiveness of radar configurations for such applications as [16]. Radar positioning is crucial for pothole detection to ensure optimum signals can be acquired. Several research exploring vehicle-mounted radar, such as Srivastava *et al.* [6] used a front-mounted radar setup, emphasising its effectiveness in estimating pothole characteristics, particularly for triangular cross-sections. Meanwhile, Ameli developed a pothole detection system, employing millimetre wave (mmWave) technology with a frequency modulated continuous waveform (FMCW) radar mounted under the car [7]. Valuyskiy *et al.* [8] investigated obstacle reflection properties, aligning with the radar module setup of this proposed work, aiming to enhance obstacle detection algorithms in advanced driver assistance systems (ADAS) simulations.

Prior research utilising a ground-penetrating radar (GPR) has also shown a promising result in detecting road defects like potholes [17]-[19]. Liang *et al.* [9] automated distress classification using 3D-GPR and neural networks, indicating enhanced road maintenance potential. Next, Zhao *et al.* [10] demonstrated GPR's effectiveness in non-contact terrain sensing, including pothole detection. Besides, Wu *et al.* [11] highlighted low-terahertz radar's superior capabilities in detecting road potholes, laying a robust groundwork for radar-based pothole detection methods. GPR feasibility for various road defects supports radar's viability for pothole sensing in this study [15], [17]-[20]. In summary, these diverse studies underscore the vast potential of radar technology in effectively sensing and analyzing road defects. These findings provide a robust foundation for our research, in terms of radar's positioning, operations and processing.

2.2. Signal feature processing and extraction

Feature extraction is pivotal in bridging the gap between raw data and effective sensing [21]-[25], including radar signal processing. Numerous studies spanning academia and industry consistently underscore its indispensable role in boosting detection accuracy. Shao *et al.* [26] introduced a method for classifying radar jamming signals, emphasizing the necessity of feature extraction for machine-learning-friendly data. Ritu *et al.* [27] have utilized signal and spectral features to improve underwater acoustic target detection.

Various works employed PSD feature extraction, which, as demonstrated by Uddin *et al.* [28] and Yesilli *et al.* [29] aids in anomaly detection and signal-based classification. Uddin *et al.* [28] applied PSD analysis to amateur drone detection, while Yesilli *et al.* [29] used it for machining chatter detection. Li *et al.* [30] pioneered PSD analysis for subsurface distress detection using GPR with deep learning. Similarly, Li *et al.* [31] emphasized PSD analysis's role in enhancing automotive radar systems, particularly in range-Doppler processing, object detection, and noise reduction for road condition detection. These studies collectively highlight the significance of PSD analysis, spectral feature extraction, and classification techniques in signal analysis across domains. This aligns with our approach of using radar data features for pothole sensing, affirming the robustness and versatility of feature extraction methods in signal classification.

2.3. Classification using k-nearest neighbors

Drawing inspiration from related research, such as motor failure identification in unmanned aerial vehicles (UAVs) and radar emitter classification, we recognise the adaptability and potential of KNN models in signal-based classification tasks [32]-[38]. Even though these studies differ from ours, they offer valuable

insights as we navigate the uncharted domain of radar-based pothole detection and classification. The choice of KNN models reflects the pioneering nature of this study, given the absence of prior work in radar-based pothole sensing. Starting with a well-established algorithm allows us to explore feasibility without undue complexity and provides a benchmark for future comparisons and improvements.

3. METHOD

3.1. Data acquisition

The experimental configuration for detecting potholes involved the assessment of pavement surfaces, with and without potholes, utilising a 24 GHz K-LC2 RFbeam radar module. This radar module is a commercially available 2×4 patch Doppler radar with a maximum effective isotropic radiated power (EIRP) of 15 dBm. The radar transceiver operated at a frequency of 24.125 GHz, featuring a 3 dB beamwidth of 80 degrees horizontally and 45 degrees vertically. Integration of the K-LC2 radar module with the RFbeam ST100 facilitated a connection to the acquisition software, RFbeam SignalViewer, via a USB cable.

The unit was installed at the front of the vehicle, positioned at a height of one meter and inclined at a 45-degree angle. For this investigation, a sedan automobile was employed with the speed of 30 km/h. Data was taken over as asphalt surface, pothole, and non-pothole. In total of 200 dataset consisted of 50% pothole and 50% non-pothole. Pothole data was take over 10 potholes and 10 times each. Meanwhile, non-pothole data was taken over a stratch of road and segmented to 100 dataset. The data acquisition setup is shown in Figure 1.
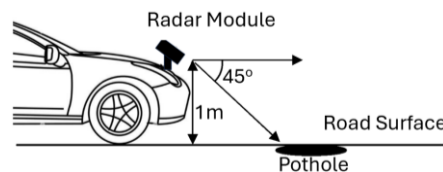

Figure 1. Data acquisition setup

3.2. Doppler signal processing

Figure 2 illustrates the workflow of the proposed pothole sensing. Raw radar signals were initially captured and stored in *.wav format. To enable subsequent analysis, MATLAB R2022b was employed to transform these signals into interpretable time domain values. The time domain signal was filtered and segmented to 1000 sample points each. The signal length is unified to prevent bias in analysis brought on by longer signals. Following this, the time domain waveforms underwent a transformation into a PSD. The PSD was computed using a discrete Fourier transform (DFT) with 256 points.
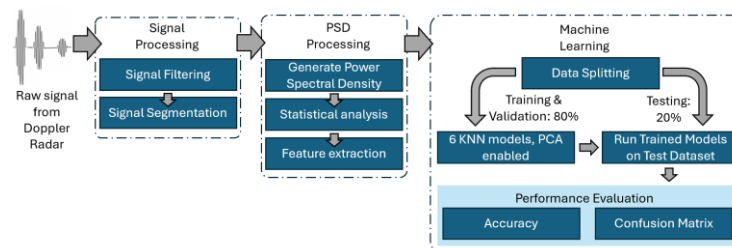

Figure 2. Block diagram the proposed of pothole sensing

The resulting PSD was statistically analysed on spectral centroid, spectral spread, spectral skewness, spectral kurtosis, spectral entropy, spectral roll-off and spectral flatness. Features from the spectral analysis were extracted and applied with KKN for classification. Table 1 tabulated spectral features utilised for the classification. In this study, we employ the MATLAB classification learner app for classification. While classification models like Naïve-Bayes, support vector machine, and decision trees are prevalent in machine learning, we focused on fusing KNN models with radar data for road condition classification ventures into unexplored territory.

3.3. Spectral analysis

Signals in the frequency domain were analysed and transformed into PSD, yielding PSD representations for both potholes and non-potholes. These PSDs enhanced insights into the dynamic interplay between Doppler signal magnitude and frequency. However, the conventional approach of peak distinction proved inadequate in categorising behaviour. Consequently, features were extracted from the PSDs, including spectral centroid, spread, skewness, kurtosis, entropy, roll-off, flatness, and total power, as detailed in Table 1.

Table 1. Feature extracted from PSD

Features list	Definition	Corresponding equation
Spectral centroid	A measure in spectral analysis pinpointing the power spectrum's center of mass. For radar, it identifies the dominant frequency, indicating road surface characteristics like smoothness or roughness.	$\mu_f = \dfrac{\sum(f_i \cdot X_i{}^2)}{\sum X_i{}^2}$
Spectral spread	Describes the width of the power spectrum distribution, assessing variability in road conditions. A broader spread suggests varying surface textures, including potholes or rough patches.	$\sigma_f = \sqrt{\dfrac{\sum((f_i - \mu_f)^2 \cdot X_i{}^2)}{\sum X_i{}^2}}$
Spectral skewness	Measures power spectrum distribution's asymmetry, indicating skew towards higher or lower frequencies. It hints at road surface uniformity or unevenness and damage.	$\gamma_f = \dfrac{\sum((f_i - \mu_f)^3 \cdot X_i{}^2)}{\sigma_f{}^3}$
Spectral kurtosis	Quantifies power spectrum "tailedness" compared to normal distribution. Higher values suggest sharp peaks, potentially corresponding to road irregularities like potholes.	$\kappa_f = \dfrac{\sum((f_i - \mu_f)^4 \cdot X_i{}^2)}{\sigma_f{}^4}$
Spectral entropy	Gauges randomness in the power spectrum, assessing frequency diversity in radar data. High entropy implies diverse road textures or conditions.	$\sum\limits_{n=1}^{R_t} M_t[n] = 0.85 \sum\limits_{n=1}^{N} M_t[n]$
Spectral roll-off	Identifies the frequency where a specific percentage of spectral energy concentrates. In road analysis, it reveals where vital spectral information lies, with lower values indicating energy concentration at lower frequencies, possibly linked to road issues.	$H_f = -\Sigma(P_i \cdot log(P_i))$
Spectral flatness	Measures tonal characteristics in a power spectrum, differentiating between uniform and noisy signals. High values suggest even energy distribution and a uniform road surface, while low values indicate energy concentration and potential road irregularities or noise.	$F_f = \dfrac{GM}{AM} = \dfrac{(\Pi_i \cdot X_i)^{1/N}}{\frac{1}{N}(\Sigma X_i)}$

Where X_i is the corresponding spectral coefficients, f_i is the frequency μ_f and σ_f is the spectral centroid and spectral spread, respectively, σ is given as the standard deviation (SD) of the spectral distribution, γ_f represents spectral skewness, κ_f represents the spectral kurtosis, M_t denotes the value for spectral roll-off, H_f denoted as spectral entropy, and F_f represents spectral flatness.

3.4. Classification using k-nearest neighbors machine learning

In this study, radar data was divided into training and testing datasets using an 80-20 split, and the KNN algorithm was employed with a range of KNN variants-coarse KNN (CKNN), cosine KNN (CosKNN), cubic KNN (cubKNN), fine KNN (fKNN), medium KNN (mKNN), and weighted KNN (wKNN). The extracted features as per Table 1 was employed to enhance the data preprocessing and feature extraction stages. By enabling PCA, the dimensionality of the feature space was effectively reduced, aiding in the mitigation of potential overfitting issues while maintaining data integrity.

The features were integrated into the KNN classification algorithm, with six KNN models applied, each differing in granularity and flexibility. The dataset consisted of 44.05% pothole data and 55.94% non-pothole data, reflecting real-world conditions. This comprehensive approach leveraged distinct KNN variants and spectral features to effectively differentiate between the two conditions. Later in section 4, there is a table showing the feature comparison between the six KNN models available in MATLAB along with their performance.

4. RESULTS AND DISCUSSION

This section discusses the results of spectral analyses done on the positive-side PSD of each collected sample. The analysis was divided into two, which were; i) spectral statistical analysis and ii) KNN model classifications.

4.1. Spectral analysis

The spectral analysis was mathematically computed over 100 readings, as per Table 1, for all seven features. Next, each feature was calculated for mean and SD. Analysis for each feature is discussed in the following subsections.

4.1.1. Spectral centroid

Figure 3 presents the spectral centroid plot. The spectral centroid plots reveal distinct distribution patterns for two scenarios. In the non-pothole road scenario, the mean spectral centroid is 891.37 with SD of 152.55, spanning from around 442.13 to 1050.56 Hz, forming a relatively symmetrical distribution concentrated in the mid to high range between 900 to 1000 Hz, with few outliers indicating unusual events. In contrast, the pothole road scenario exhibits a mean spectral centroid of 632.62 with an SD of 233.62, ranging from approximately 199.10 to 1132.32, showing a bimodal distribution. The first scenario demonstrates a concentrated distribution with a higher mean and lower SD. The second scenario displays a broader spread with a lower mean and higher SD, suggesting more variability in the acoustic signal landscape due to potholes.

4.1.2. Spectral spread

Meanwhile, observation on the spectral centroid plot in Figure 4 demonstrates stable frequency distributions for a non-pothole, with a mean spectral spread of 384.42 and an SD of 76.33, while pothole-ridden roads exhibit wider frequency variations, featuring a higher mean spectral spread of 486.78 with a larger SD of 240.00. The presence of outliers exceeding 600 and even reaching as high as 1393.08 in pothole conditions reflects the impact of road disruptions. Non-pothole conditions show a more consistent audio profile with infrequent outliers. In summary, the non-pothole road condition exhibits a more consistent and stable audio characteristic with a lower mean and SD, while the pothole condition shows a broader range of frequency variation, a higher mean, and more significant variability, primarily due to the impacts of potholes. These differences underscore the distinct audio signatures associated with these road conditions and emphasize the potential hazards of potholes in road safety and infrastructure maintenance.
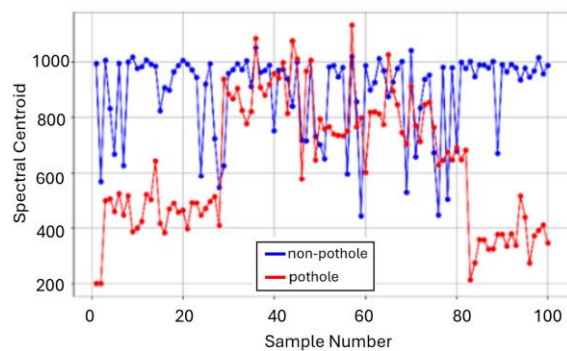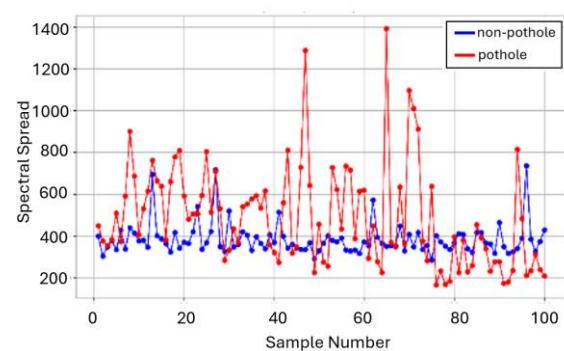

Figure 3. Spectral centroid plot

Figure 4. Spectral spread plot

4.1.3. Spectral skewness

Next, Figure 5 depicts the spectral skewness. Comparison of spectral skewness plots between non-pothole and pothole-ridden roads reveals distinct patterns in spectral energy distribution. In the non-pothole scenario, the mean skewness is 6.68, with a low SD at 0.57, indicating a consistent energy distribution across frequencies 5.6 to 7.8 Hz. Conversely, the pothole-ridden road has a higher mean skewness of 7.34 and a larger SD of 1.35, indicating wider energy distribution variations between 4.3 and 11.2. Positive skewness in the latter suggests a bias towards higher frequencies, indicative of deviations like potholes. Overall, the non-pothole exhibits balanced energy distribution, while the pothole-ridden shows significant irregularities.

4.1.4. Spectral kurtosis

The spectral kurtosis plot is presented in Figure 6. In spectral kurtosis evaluation for non-pothole road conditions, values exhibit moderate variability between 35.87 and 81.01, with a mean of roughly 49.43 and SD of 8.63. Clusters occur across lower and higher ranges, implying variations. Notable outliers signify potential road irregularities, warranting further statistical and temporal analysis to understand underlying patterns critical for road safety assessment. Conversely, in pothole scenarios, spectral kurtosis values range from 22.55 to 125.64, with a mean of about 60.76 and SD of 21.64. The higher mean and larger SD compared to even road conditions highlight increased variability and impulsive events linked to potholes. Spectral kurtosis values lack distinct clustering patterns but exhibit multiple peaks, indicating diverse types and intensities of potholes along the road. Severe outliers suggest particularly rough road sections.
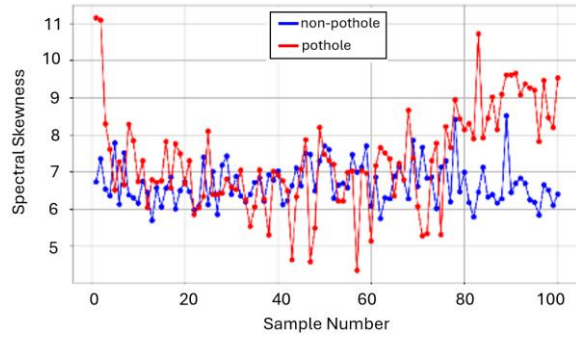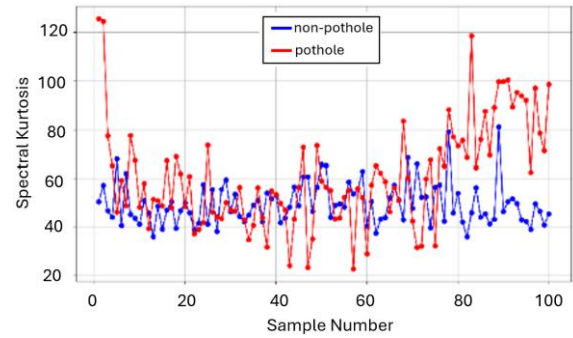
Figure 5. Spectral skewness

Figure 6. Spectral surtosis

4.1.5. Spectral entropy

Figure 7 plots the spectral entropy for two distinct road conditions: non-pothole road and pothole. In the non-pothole road scenario, spectral entropy values are normally distributed, with a mean of 2.25 and SD of 0.24. This trend represents a consistent and stable road environment, with a subtle upward trend in complexity over time. Conversely, the pothole case reveals a wider, more variable distribution of spectral entropy values, with a mean of 2.03 and SD of 0.56. This indicates frequent fluctuations and unpredictability in road conditions, particularly in areas with potholes. Overall, the non-pothole road case signifies a stable road condition with a gradual increase in complexity. On the other hand, the pothole scenario reflects highly variable and unpredictable road conditions, primarily due to potholes.

4.1.6. Spectral roll-off

The spectral roll-off plots in Figure 8 for non-pothole and pothole depict distinct audio characteristics. The plot displays a more focused distribution in the non-pothole road case, with a mean spectral roll-off of 1140.40 Hz and SD of 184.50 Hz. The primary peak is at 1205.86 Hz, indicating a concentration of spectral energy in higher frequencies. Conversely, the pothole exhibits a broader and more varied distribution, with a mean spectral roll-off of 933.68 Hz and a higher SD of 385.73 Hz. Multiple peaks are evident, with the most prominent at 861.33 Hz, likely related to the existence of potholes. These findings highlight the differences between the two scenarios, with non-pothole roads featuring a narrower and higher-frequency focus, while pothole exhibits a broader spectrum of audio characteristics, particularly in mid-frequency components. The mean and SD values underscore these distinctions and provide valuable insights into the audio profiles of these scenarios.
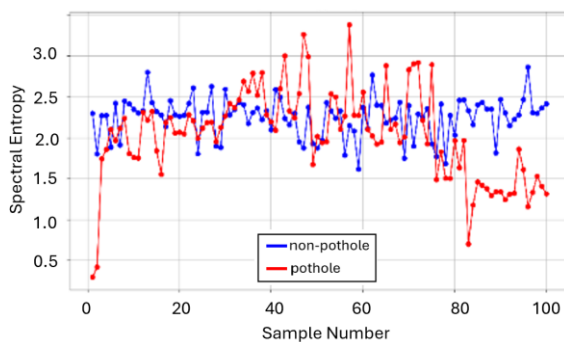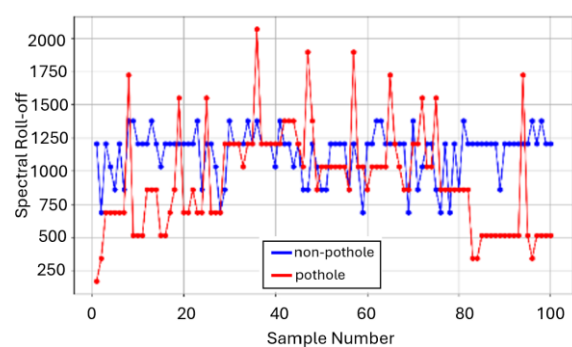

Figure 7. Spectral entropy

Figure 8. Spectral roll-off

4.1.7. Spectral flatness

Finally, Figure 9 illustrates the spectral flatness. The spectral flatness analysis reveals notable differences between the non-pothole road and pothole cases. For the non-pothole road, spectral flatness values mostly range from 0.001 to 0.0048, with moderate fluctuations around the mean of 0.00186 and a low SD of 0.00062, indicating a stable audio signal with minor variations. Conversely, the pothole case exhibits wider fluctuations, ranging from 0.00027 to 0.01426. The mean spectral flatness is 0.00255, with a

significantly higher SD of 0.00232, suggesting increased variability in the audio signal due to potholes. These results imply that the non-pothole road case exhibits a relatively stable and consistent audio signal. In contrast, the pothole case demonstrates more significant variability and distinctive features in the spectral flatness plot, likely related to the presence of potholes.
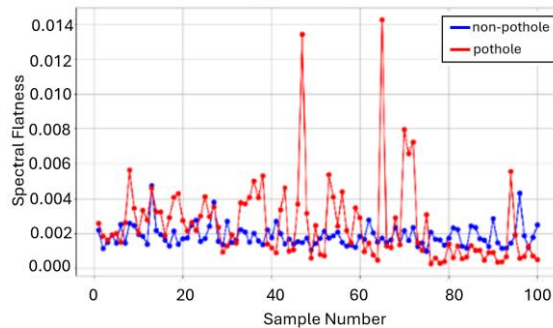

Figure 9. Spectral flatness

4.2. K-nearest neighbors models classification
4.2.1. Accuracy evaluation

By examining the machine learning model's performance on the test dataset provides valuable insights into the efficacy of distinct KNN algorithm variants for road condition classification using radar data. Table 2 compares the KNN models analysed. Among the KNN variants, fine KNN stands out as the most adaptable, achieving an accuracy of 95.83%, followed by Weighted KNN with an accuracy of 94.44%. The adaptability of fine KNN is evident in its ability to select the most suitable distance metric for the specific characteristics of potholes and non-potholes datasets. This adaptability ensures that the model accurately captures the true relationships in the data, leading to more precise classifications.

Table 2. Comparison between KNN models, features, and results

KNN variant	Number of neighbours	Distance metric	Distance weight	Accuracy (training) (%)	Accuracy (test) (%)
Coarse KNN	100	Euclidean	Equal	78.47	76.39
Cosine KNN	10	Cosine	Equal	84.03	91.67
Cubic KNN	10	Minkowski (cubic)	Equal	87.50	90.28
Fine KNN	1	Euclidean	Equal	89.58	95.83
Medium KNN	10	Euclidean	Equal	86.81	90.28
Weighted KNN	10	Euclidean	Equal	85.58	94.44

Additionally, fine-tuning optimises the k value, achieving the right balance between underfitting and overfitting. This optimisation is crucial as it ensures that the model generalises well to new, unseen data while minimising the impact of noise. By handling noise more effectively, fine KNN reduces the likelihood of misclassifications due to anomalous data points.

Overall, this evaluation elucidates the substantial impact of algorithm choice on the model's capacity to distinguish between different road conditions accurately. The superior performance of fine KNN underscores the importance of fine-tuning machine learning models to enhance their accuracy and robustness in practical applications. The results highlight that selecting the right algorithm and optimising its parameters are critical to developing effective radar-based road condition classification systems.

4.2.2. Confusion matrix

Next, the analysis was conducted over confusion matrices. The confusion matrices reveal the performance of various KNN models in distinguishing between non-pothole road conditions and potholes. Accompanied by corresponding accuracy metrics, these matrices offer valuable insights into each model's proficiency. Figure 10 depicts the test confusion matrix for all the KNNs analyzed.

Coarse KNN, as shown in Figure 10(a), displays the lowest accuracy of 76.39%. This model classifies non-pothole conditions with a 97.5% true positive rate (TPR) and a 2.5% false negative rate (FNR).

However, it struggles significantly with pothole classification, producing a 50%-50% ratio between TPR and FNR for the pothole scenario, indicating a high level of misclassification.

Cosine KNN, illustrated in Figure 10(b), shows a lower TPR of 2.5% for non-pothole conditions but a better TPR of 37.5% for potholes. This indicates an improvement in identifying potholes compared to coarse KNN but at the cost of non-pothole classification accuracy. Cubic KNN, presented in Figure 10(c), has a similar TPR for non-pothole conditions as coarse KNN at 97.5%. However, it categorizes non-pothole conditions correctly 81.2% of the time, with a misclassification rate of 18.8% for non-pothole scenarios. The result indicates a better balance but also highlights significant room for improvement in accuracy, suggesting potential for further research and development.

Fine KNN, depicted in Figure 10(d), emerges as the most effective model with an accuracy of 95.83%. It maintains a high TPR for non-potholes, similar to coarse KNN and cubic KNN, but excels in separating non-pothole conditions with a 93.8% TPR for potholes. This demonstrates its superior ability to classify both conditions accurately.

Medium KNN, shown in Figure 10(e), achieves an 81.2% TPR for non-pothole conditions, indicating a balanced but less accurate performance than fine KNN. Weighted KNN, illustrated in Figure 10(f), follows closely behind Fine KNN with a 90.6% TPR for non-pothole conditions, demonstrating its effectiveness in classification but still slightly less accurate than fine KNN. To sum up, fine KNN, weighted KNN, and cosine KNN show promising accuracy capacities compared to all six KNN models analyzed. The confusion matrices provide detailed insights into each model's ability to classify road conditions accurately, aiding in selecting the most appropriate model for specific road condition differentiation requirements. Fine KNN stands out as the most proficient, followed by Weighted KNN, due to their higher overall accuracy and better handling of non-pothole and pothole classifications.
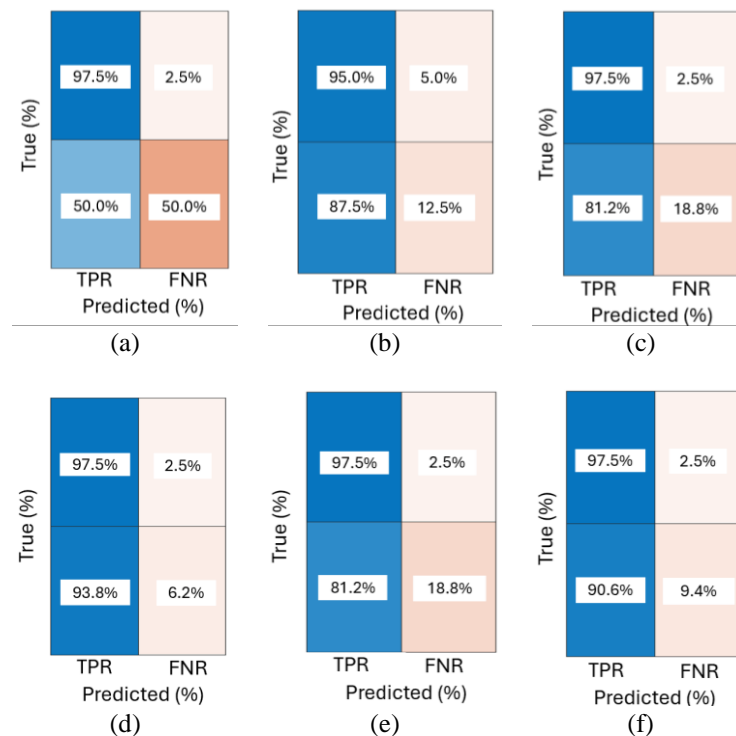

Figure 10. Test confusion matrix; (a) coarse KNN, (b) cosine KNN, (c) cubic KNN, (d) fine KNN, (e) medium KNN, and (f) weighted KNN

5.   CONCLUSION

The research aimed to develop machine learning models for classifying road conditions using radar data, focusing on differentiating between potholes and non-pothole road conditions. The process involved processing audio data from radar sensors mounted on vehicles to extract key audio features through PSD analysis. A comprehensive analysis of various KNN algorithm variants was conducted to determine their effectiveness in classification. Fine KNN emerged as the most successful, achieving 95.83% accuracy. Confusion matrices provided detailed insights into each model's performance, revealing patterns of true

positives, true negatives, false positives, and false negatives. This research highlights the potential of machine learning in accurately categorizing road conditions, emphasizing the role of algorithmic choices and parameter optimization in achieving precise results.

ACKNOWLEDGEMENTS

REFERENCES

[1] The Global Economy, "Roads Quality - Country Rankings," *TheGlobalEconomy.com*. [Online]. Available: https://www.theglobaleconomy.com/rankings/roads_quality. (Date accessed: Feb. 24, 2024).
[2] A. Y. Her, W. K. Yew, P. J. Yew, and M. C. J. Ying, "Real-time pothole detection system on vehicle using improved YOLOv5 in Malaysia," in *IECON Proceedings (Industrial Electronics Conference)*, IEEE, Oct. 2022, pp. 1–5, doi: 10.1109/IECON49645.2022.9968423.
[3] W.-H. Chen, "Visible & Thermal Imaging and Deep Learning Based Approach for Automated Robust Detection of Potholes to Prioritize Highway Maintenance," Colorado State University, Fort Collins, Colorado, 2023.
[4] P. A. Chitale, K. Y. Kekre, H. R. Shenai, R. Karani, and J. P. Gala, "Pothole Detection and Dimension Estimation System using Deep Learning (YOLO) and Image Processing," in *International Conference Image and Vision Computing New Zealand*, IEEE, Nov. 2020, pp. 1–6, doi: 10.1109/IVCNZ51579.2020.9290547.
[5] L. Rufei, Y. Jiben, R. Hongwei, C. Bori, and C. Chenhao, "Research on a pavement pothole extraction method based on vehicle-borne continuous laser scanning point cloud," *Measurement Science and Technology*, vol. 33, no. 11, p. 115204, Nov. 2022, doi: 10.1088/1361-6501/ac875c.
[6] A. Srivastava, A. Goyal, and S. S. Ram, "Radar cross-section of potholes at automotive radar frequencies," in *2020 IEEE International Radar Conference, RADAR 2020*, IEEE, Apr. 2020, pp. 483–488, doi: 10.1109/RADAR42522.2020.9114858.
[7] S. Ameli, "Road Condition Sensing Using Deep Learning and Wireless Signals," University of Waterloo, Waterloo, Ontario, Canada, 2020.
[8] D. V. Valuyskiy, A. A. Panarina, S. V. Vityazev, and V. V. Vityazev, "Test bench development for signal registration in millimeter wave automotive radars," *IOP Conference Series: Materials Science and Engineering*, vol. 534, no. 1, pp. 1-5, May 2019, doi: 10.1088/1757-899X/534/1/012020.
[9] X. Liang, X. Yu, C. Chen, Y. Jin, and J. Huang, "Automatic Classification of Pavement Distress Using 3D Ground-Penetrating Radar and Deep Convolutional Neural Network," *IEEE Transactions on Intelligent Transportation Systems*, vol. 23, no. 11, pp. 22269–22277, Nov. 2022, doi: 10.1109/TITS.2022.3197712.
[10] L. Zhao, J. Zhang, S. Jiao, T. Zheng, J. Li, and T. Zhao, "Ground surface detection method using ground penetrating radar signal for sugarcane harvester base-cutter control," *Biosystems Engineering*, vol. 219, pp. 103–123, Jul. 2022, doi: 10.1016/j.biosystemseng.2022.04.024.
[11] H. Wu, F. Qi, and J. Wang, "Low-Terahertz Radar Image Analysis for Road Obstacles," in *Proceedings of the 33rd Chinese Control and Decision Conference, CCDC 2021*, IEEE, May 2021, pp. 7595–7598, doi: 10.1109/CCDC52312.2021.9601753.
[12] K. Bhavana, S. Munappa, K. D. Bhavani, P. Deshmanth, A. Swathi, and S. R. Vanga, "Automatic Pothole and Humps on Roads Detection and Notification Alert," in *Proceedings of the 2023 2nd International Conference on Electronics and Renewable Systems, ICEARS 2023*, IEEE, Mar. 2023, pp. 1–6, doi: 10.1109/ICEARS56392.2023.10085086.
[13] T. Kalushkov, G. Shipkovenski, E. Petkov, and R. Radoeva, "Accelerometer Sensor Network for Reliable Pothole Detection," in *ISMSIT 2021 - 5th International Symposium on Multidisciplinary Studies and Innovative Technologies, Proceedings*, IEEE, Oct. 2021, pp. 57–61, doi: 10.1109/ISMSIT52890.2021.9604743.
[14] L. R. L. V. Raj, A. Jidin, C. W. M. F. C. W. M. Zalani, K. A. Karim, G. W. Yen, and M. H. Jopri, "Improved performance of DTC of five-phase induction machines," in *Proceedings of the 2013 IEEE 7th International Power Engineering and Optimization Conference, PEOCO 2013*, IEEE, Jun. 2013, pp. 613–618, doi: 10.1109/PEOCO.2013.6564621.
[15] Q. Cao and I. L. Al-Qadi, "Effect of moisture content on calculated dielectric properties of asphalt concrete pavements from ground-penetrating radar measurements," *Remote Sensing*, vol. 14, no. 1, pp. 1-16, Dec. 2022, doi: 10.3390/rs14010034.
[16] K. K. M. Shariff, Z. Awang, I. Pasya, and S. A. M. Al Junid, "Theoretical Accuracy Analysis of a 4-Beam Speed- Over-Ground Radar on Uneven Surface," in *RFM 2018 - 2018 IEEE International RF and Microwave Conference, Proceedings*, IEEE, Dec. 2018, pp. 325–328, doi: 10.1109/RFM.2018.8846527.
[17] S. Li *et al.*, "Detection of concealed cracks from ground penetrating radar images based on deep learning algorithm," *Construction and Building Materials*, vol. 273, pp. 1-14, Mar. 2021, doi: 10.1016/j.conbuildmat.2020.121949.
[18] J. Gao, D. Yuan, Z. Tong, J. Yang, and D. Yu, "Autonomous pavement distress detection using ground penetrating radar and region-based deep learning," *Measurement: Journal of the International Measurement Confederation*, vol. 164, pp. 1-14, Nov. 2020, doi: 10.1016/j.measurement.2020.108077.
[19] M. E. Torbaghan, W. Li, N. Metje, M. Burrow, D. N. Chapman, and C. D. F. Rogers, "Automated detection of cracks in roads using ground penetrating radar," *Journal of Applied Geophysics*, vol. 179, pp. 1-40, Aug. 2020, doi: 10.1016/j.jappgeo.2020.104118.
[20] R. S. Rodrigues, M. Pasin, A. Kozakevicius, and V. Monego, "Pothole detection in asphalt: An automated approach to threshold computation based on the haar wavelet transform," in *Proceedings - International Computer Software and Applications Conference*, IEEE, Jul. 2019, pp. 306–315, doi: 10.1109/COMPSAC.2019.00053.
[21] P. Kokate, S. Pancholi, and A. M. Joshi, "Classification of Upper Arm Movements from EEG signals using Machine Learning with ICA Analysis," *arXiv*, pp. 1–41, 2021, doi: 10.48550/arXiv.2107.08514.
[22] A. Paul *et al.*, "Development Of Automated Cardiac Arrhythmia Detection Methods Using Single Channel ECG Signal," *arXiv*, pp. 1–17, 2023, doi: 10.48550/arXiv.2308.02405.

[23] S. M. Redwan, M. P. Uddin, A. Ulhaq, M. I. Sharif, and G. Krishnamoorthy, "Power spectral density-based resting-state EEG classification of first-episode psychosis," *Scientific Reports*, vol. 14, no. 1, p. 15154, 2024, doi: 10.1038/s41598-024-66110-0.
[24] G. P. Kafentzis, S. Tetsing, J. Brew, L. Jover, and M. Galvosas, "Predicting Tuberculosis from Real-World Cough Audio Recordings and Metadata," *arXiv*, pp. 1–13, 2023, doi: 10.48550/arXiv.2307.0484.
[25] T. N. S. T. Zawawi, A. R. Abdullah, M. H. Jopri, T. Sutikno, N. M. Saad, and R. Sudirman, "A review of electromyography signal analysis techniques for musculoskeletal disorders," *Indonesian Journal of Electrical Engineering and Computer Science*, vol. 11, no. 3, pp. 1136–1146, Jul. 2018, doi: 10.11591/ijeecs.v11.i3.pp1136-1146.
[26] G. Shao, Y. Chen, and Y. Wei, "Deep Fusion for Radar Jamming Signal Classification Based on CNN," *IEEE Access*, vol. 8, pp. 117236–117244, 2020, doi: 10.1109/ACCESS.2020.3004188.
[27] J. Ritu, E. Barnes, R. Martell, A. Van Dine, and J. Peeples, "Histogram Layer Time Delay Neural Networks for Passive Sonar Classification," in *IEEE Workshop on Applications of Signal Processing to Audio and Acoustics*, 2023, doi: 10.1109/WASPAA58266.2023.10248102.
[28] Z. Uddin, M. Altaf, M. Bilal, L. Nkenyereye, and A. K. Bashir, "Amateur Drones Detection: A machine learning approach utilizing the acoustic signals in the presence of strong interference," *Computer Communications*, vol. 154, pp. 236–245, Mar. 2020, doi: 10.1016/j.comcom.2020.02.065.
[29] M. C. Yesilli, F. A. Khasawneh, and B. P. Mann, "Transfer learning for autonomous chatter detection in machining," *Journal of Manufacturing Processes*, vol. 80, pp. 1–27, Aug. 2022, doi: 10.1016/j.jmapro.2022.05.037.
[30] Y. Li, C. Liu, G. Yue, Q. Gao, and Y. Du, "Deep learning-based pavement subsurface distress detection via ground penetrating radar data," *Automation in Construction*, vol. 142, p. 104516, Oct. 2022, doi: 10.1016/j.autcon.2022.104516.
[31] X. Li, X. Wang, Q. Yang, and S. Fu, "Signal Processing for TDM MIMO FMCW Millimeter-Wave Radar Sensors," *IEEE Access*, vol. 9, pp. 167959–167971, 2021, doi: 10.1109/ACCESS.2021.3137387.
[32] A. Altinors, F. Yol, and O. Yaman, "A sound based method for fault detection with statistical feature extraction in UAV motors," *Applied Acoustics*, vol. 183, pp. 1-14, Dec. 2021, doi: 10.1016/j.apacoust.2021.108325.
[33] Z. Seddighi, M. R. Ahmadzadeh, and M. R. Taban, "Radar signals classification using energytime-frequency distribution features," *IET Radar, Sonar and Navigation*, vol. 14, no. 5, pp. 707–715, May 2020, doi: 10.1049/iet-rsn.2019.0331.
[34] X. Li, Z. Liu, Z. Huang, and W. Liu, "Radar Emitter Classification with Attention-Based Multi-RNNs," *IEEE Communications Letters*, vol. 24, no. 9, pp. 2000–2004, Sep. 2020, doi: 10.1109/LCOMM.2020.2995842.
[35] M. Ezuma, C. K. Anjinappa, M. Funderburk, and I. Guvenc, "Radar Cross Section Based Statistical Recognition of UAVs at Microwave Frequencies," *IEEE Transactions on Aerospace and Electronic Systems*, vol. 58, no. 1, pp. 27–46, Feb. 2022, doi: 10.1109/TAES.2021.3096875.
[36] N. A. J. Gnamele, Y. B. Ouattara, T. A. Kobea, G. Baudoin, and J. M. Laheurte, "KNN and SVM classification for chainsaw sound identification in the forest areas," *International Journal of Advanced Computer Science and Applications*, vol. 10, no. 12, pp. 531–536, 2019, doi: 10.14569/ijacsa.2019.0101270.
[37] M. H. Jopri, M. R. Ab Ghaiii, A. R. Abdullah, M. Manap, T. Sutikno, and J. Too, "K-nearest neighbor and naïve bayes based diagnostic analytic of harmonic source identification," *Bulletin of Electrical Engineering and Informatics*, vol. 9, no. 6, pp. 2650–2657, Dec. 2020, doi: 10.11591/eei.v9i6.2685.
[38] M. H. Jopri, A. R. Abdullah, M. Manap, M. B. N. Shah, T. Sutikno, and J. Too, "Linear discriminate analysis and K-nearest neighbor based diagnostic analytic of harmonic source identification," *Bulletin of Electrical Engineering and Informatics*, vol. 10, no. 1, pp. 171–178, Feb. 2021, doi: 10.11591/eei.v10i1.2686.

BIOGRAPHIES OF AUTHORS

Muhammad Aiman Dani Asmadi ⓘ 🕸 ˢᶜ ▷ is currently pursuing Masters in Electronics and Computer Engineering in Faculty of Electronics and Computer Technology and Engineering (FTKEK), Universiti Teknikal Malaysia Melaka (UTeM). He holds a Bachelors of Mechanical Precision Engineering from University of Technology Malaysia (UTM), Malaysia in 2020. His research includes radars, signal processing, and machine learning. He can be contacted at email: m022220001@student.utem.edu.my.

Suraya Zainuddin ⓘ 🕸 ˢᶜ ▷ is a Senior Lecturer in Faculty of Electronics and Computer Technology and Engineering (FTKEK), Universiti Teknikal Malaysia Melaka (UTeM). She received the Bachelor of Engineering (Electrical-Telecommunication) from Universiti Teknologi Malaysia (UTM) in 2003, M.Sc. in Telecommunication and Information Engineering in from Universiti Teknologi MARA (UiTM) in 2015 and Ph.D. in Electrical Engineering from the similar university in 2020. Her main research areas involved the studies in multiple-input multiple-output (MIMO) radar, radar system and application, signal processing, and radar detection. She can be contacted at email: suraya@utem.edu.my.

Haslinah Mohd Nasir 🆔 🔍 SC ◐ is a Lecturer in Faculty of Electronics and Computer Technology and Engineering (FTKEK), Universiti Teknikal Malaysia Melaka (UTeM). received her bachelor's degree in electrical - Electronic Engineering (2008) from Universiti Teknologi Malaysia (UTM), M.Sc. (2016) and Ph.D. (2019) in Electronic Engineering from Universiti Teknikal Malaysia Melaka (UTeM). She had 5 years (2008-2013) experience working in industry and currently a lecturer in UTeM. Her research interests include microelectronics, artificial intelligence, and biomedical. She can be contacted at email: haslinah@utem.edu.my.

Ida Syafiza Md Isa 🆔 🔍 SC ◐ obtained her Ph.D. from the University of Leeds, UK in 2020 for work on energy efficient access networks design for healthcare applications. She has research interests in network architecture design, energy efficiency, network optimization, mixed integer linear programming and healthcare systems. She has published several papers in this area. She is currently a senior lecturer in Universiti Teknikal Malaysia Melaka (UTeM), Malaysia. She can be contacted at email: idasyafiza@utem.edu.my.

Nur Emileen Abd Rashid 🆔 🔍 SC ◐ is an Associate Professor in Faculty of Electrical Engineering, Universiti Teknologi MARA (UiTM). She received the Bachelor of Engineering in Electrical Engineering (Communications) from Universiti Kebangsaan Malaysia (UKM), MSc in Telecommunications, Computer and Human Centered Engineering from University of Birmingham and Ph.D. in Electrical Engineering (Radar Technology) from the similar university. She is currently the Head for Centre of Postgraduate Studies, Faculty of Electical Engineering, UiTM. Her main research areas are radar system, classification, telecommunication signal processing, antenna, and radar detection. She can be contacted at email: emileen98@uitm.edu.my.

Idnin Pasya 🆔 🔍 SC ◐ is an Associate Professor in Department of Computer Science and Engineering, The University of Aizu, Japan. He received the Bachelor of Engineering and and Master of Engineering in Information and Communication Engineering from Tokyo Denki University in 2004 and 2006, and his Ph.D. in Communication Engineering from the same university in 2015. He previously worked at Toshiba PC and Network Corporation in Tokyo Japan from 2006-2009, and in University Teknologi MARA, Malaysia from 2010-2022, before joining University of Aizu. His main research areas are multiple-input multiple-output (MIMO) radars, ultra wide band (UWB) systems and applications, underwater antennas, and communication systems. He can be contacted at email: idnin@u-aizu.ac.jp.